White Paper:
SIMULATION OF WIND TURBINE ROTOR WITH COMPUTATIONAL FLUID DYNAMICS (CFD)

FRECON
engineering value

1.1   Introduction

Over the last decades, computational fluid dynamics has developed into a powerful tool to solve booth basic and advanced engineering problems. The field of application spans over a broad variety of topics, reaching from chemical engineering over aerodynamics to biofluid simulations.

The present paper is an example of the usage of computational fluid dynamics in wind turbine aerodynamics. It describes the development of a model to solve the flow around a wind turbine rotor in steady state conditions and rotating frame of reference. This allows a first look at the flow around a full wind turbine rotor without the usage of an expensive transient model with the advantage of only simulating a single blade. Results like pressure, velocity and vorticity distributions are analysed and discussed.

This paper is for demonstration purposes only. The used blade geometry is open to the public and has been used for CFD course purposes (Cornell University, 2018). The described method has been used as baseline for the present simulations.

1.2   Model

The blade model used for the present calculation resembles the blades of the GE 1.5XLE horizontal axis wind turbine. The three blades of the rotor have a radius of $R = 43.2\ m$ and consist of s818, s825 and s826 airfoils for the root, body and tip, respectively. The rated wind speed of this turbine is around $U_{rated} = 11.5\ m/s$, resulting in a rated power of $P_{rated} = 1.5\ MW$ (thewindpower.net, 2018). The blade geometry is shown in Figure 1.

Figure 1: Blade geometry

1.3   Computational domain

The computational domain used for the present calculations is a third of a cone shaped volume of fluid, shown in Figure 2. This volume of fluid ensures the possibility to calculate the flow around the blade in a rotating frame of reference. Periodic boundary conditions enable the modelling of two additional blades. This results in the possibility to visualize the flow around a complete rotor with three blades.
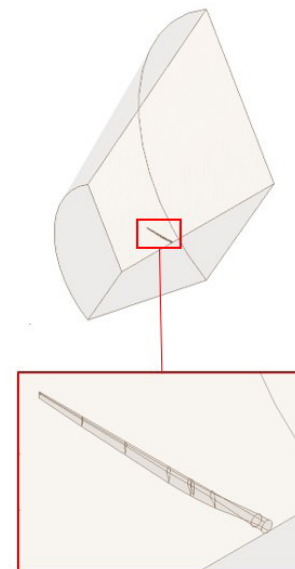

Figure 2: Computational domain

1.4   Mesh

For the present case, the grid generation is focused on the area near the blade. The following three factors are of major interest:

- The mesh on the blade surface needs to be refined sufficiently to capture the complex geometry and curvatures.
- The mesh near the blade must be refined as much as possible to resolve the flow near the blade surface.
- The overall amount of cells needs to be kept as low as possible to save computational time.

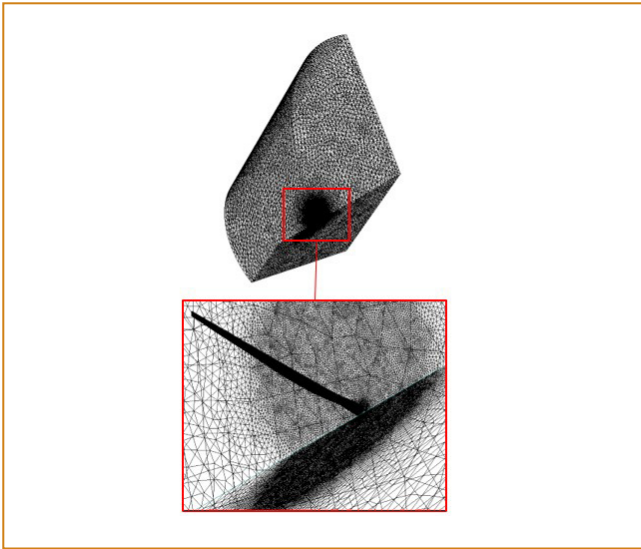The resulting mesh is shown in Figure 3.

Figure 3: Global and local mesh wire frame

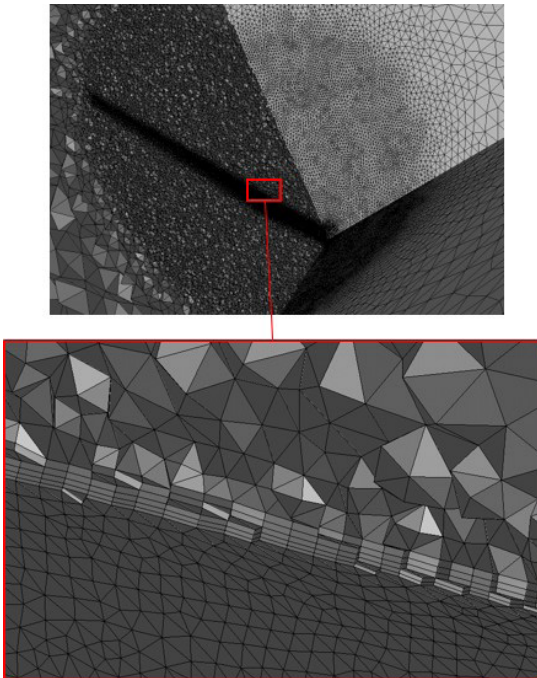A section view and zoom on the blade is shown in Figure 4.

Figure 4: Section view and zoom view of inflation layers

The local mesh refinement is visible as a circular area around the blade. To capture the flow near the blade, inflation layers are inserted on the blade surface, visible in the lower picture of Figure 4.

A mesh independent solution is ensured through a convergence study. The velocity in a stationary frame of reference is monitored at a specified point in the wake of the rotor inside the circular refinement visible in the upper picture of Figure 4.
Table 1 gives an overview of the mesh statistics of the convergence study for mesh refinement in the circular area.

Cell size $(\Delta x=\Delta y=\Delta z)$	Total amount of cells	Velocity
1000 mm	1.5 M	5.65
500 mm	5.27 M	5.637
125 mm	33.47 M	5.646

Table 1: Mesh overview for convergence study

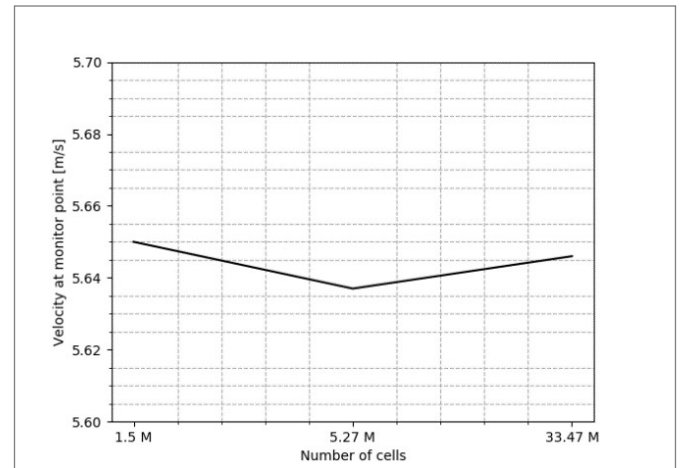The change in velocity between each refinement is shown in Figure 5.

Figure 5: Change of velocity between each refinement

With respect to the increase of cells from the second to the third refinement and the corresponding change in velocity it is assumed, that a refinement of $(\Delta x=\Delta y=\Delta z)=500\ mm$ results in a sufficient converged solution.

1.5   Model setup and boundary conditions

The model is solved in a rotating frame of reference, assuming the rotor has a rotational speed of $\omega = 1.95$ rad/s, corresponding to the maximum rotor speed (wind-turbine-models.com, 2018). With the axis of rotation in the center of the cone, which adds an additional meter to the radius of the blade, the resulting tip speed ratio is $\lambda = 7.51$.

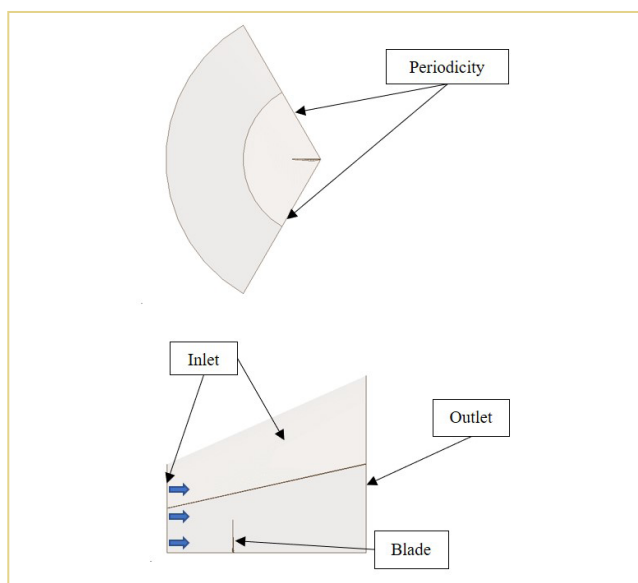The boundary conditions are described and illustrated in Figure 6.

Figure 6: Boundary conditions

The direction of the free stream velocity is indicated with arrows.
The following boundary conditions are applied:

Inlet: The inlets are defined as velocity inlets with a constant velocity of $U_\infty = 11.5\ m/s$, corresponding to the rated wind speed of the turbine.

Outlet: The outlet is defined as pressure outlet with a relative pressure of 0 Pa and placed as shown in Figure 6. The outlet is placed 3.5 rotor radii downstream the rotor plane.

Lateral boundaries: The lateral boundaries are set to be periodic boundary conditions, repeating the computational domain with respect to the selected plane.

Internal flow field: The internal flow field is initialized to have a reference pressure of 1 atm.

Blade: The blade surface is defined as no-slip wall.

1.6   Solver parameters

The flow is solved in steady-state conditions using a pseudo transient k-omega SST model.

1.7   Results

Since the blade geometry for the present simulation is a simple model, constructed from a point cloud of the three mentioned airfoils, the overall accuracy of the simulation is questionable. However, simple comparisons of characteristic aerodynamic values and flow structures show, that the model is working appropriately.

Lift- and drag coefficients: Lift- and drag forces are extracted from a section of a blade and compared to calculations performed in Xfoil. All values are calculated for the corresponding Reynolds number, based on the relative velocity experienced by the blade section and the corresponding angle of attack. Values for lift- and drag coefficients are shown in Table 2.

Airfoil	Data	C_l	C_d
S826	CFD	0.805	0.0068
	Xfoil	0.840	0.005

Table 2: Lift- and drag coefficients for s826 airfoil

The coefficients do not match completely but, keeping in mind that the blade geometry is kept simple, the difference is assumed to be sufficient for the present simulation.
The simplification of the blade geometry is visible in Figure 7, which shows a blade section with a s818 airfoil in the top and the same airfoil taken from Xfoil.
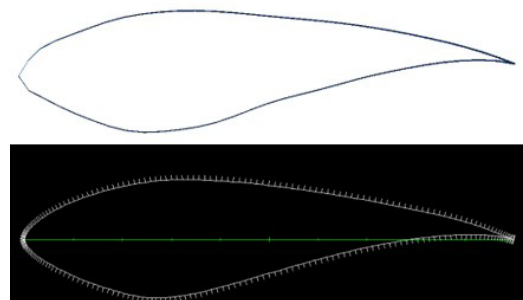

Figure 7: Comparison between airfoils for the blade gemetry (top) and xfoil airfoil (bottom)

The geometrical difference is especially visible at the leading edge of the two airfoil profiles, which is smooth for the Xfoil profile and sharp for the geometry used for the present simulation.

Rotor velocity: From Figure 8 it is visible that the rotor is experiencing a rotational motion in the clockwise direction.
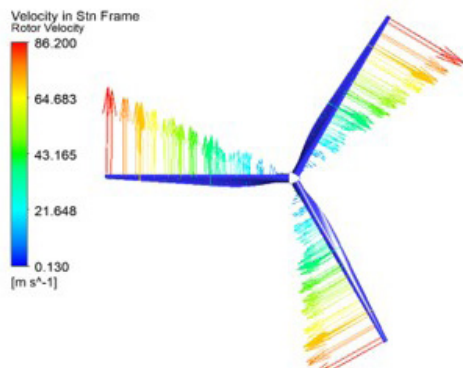

Figure 8: Rotor velocity

The coloured vectors along the blades visualize the rotational velocity of the blade. Increasing vector length indicate higher velocity. The velocity of *86.2 m/s* at the tip is in good agreement with manually calculated tip speed of *86.19 m/s*.

Flow characteristics: Figure 9 shows the pressure distribution around a section of a blade. The upper picture shows the result from CFD calculations and the lower the results from Xfoil calculations for the corresponding airfoil.
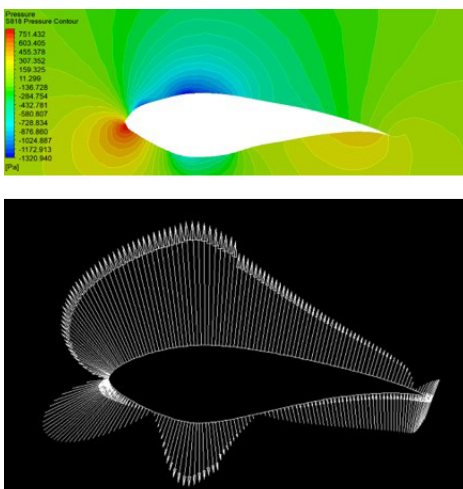

Figure 9: Pressure distribution around S818 airfoil

Pressure above and below the reference pressure are visualized with colours from red (above reference pressure) to blue (below reference pressure) in the upper picture and vectors with arrow heads pointing towards (above reference pressure) and away (below reference pressure) from the airfoil. The length of the vectors indicates the pressure magnitude.

Through visual comparison it can be concluded, that the pressure distribution of the two individual calculations of the same airfoil are in good accordance with each other.

Power output: The produced power by the rotor is calculated from the total generated torque of the three blades and found to be P_{sim} = *1.6 MW*. Comparing with the rated power of the reference turbine, a difference of 0.1 MW is observed. The difference is most probably due to the following:

- The rate wind speed of U_{rated} = *11.5 m/s* is defined to be the average wind speed at hub height of the wind turbine. The wind speed at different azimuthal positions varies in general, whereas it is uniform for the present simulation.

- The calculated power is based on the torque coming from pressure and viscous forces. The calculations do not take any other possible losses into account.
- The rotor is simulated without hub, nacelle and tower.
- The used geometry is not completely equal to the blades used for the reference turbine.

Vorticity: The vorticity distribution along the blades of the rotor and the wake downstream is shown in Figure 10.

Figure 10: Vorticity magnitude

The vorticity distribution around and downstream the wind turbine rotor gives an insight in the overall aerodynamic performance of the rotor. According to the Kutta-Joukowsky theorem, the lift force at a blade section is proportional to the free stream velocity and the circulation at that section.

Furthermore, according to Joukowsky, optimum rotors have constant circulation distribution along the span of the blade, resulting in vortices shedding from the tip and the root of the blade (von Eitzen, 2018).

In Figure 10, well defined vortex tubes are shedding from the tip of the blade. The same appears for the root of the blades. In the region near the root however, a continuous helicoida vortex region is shedded from the blade, which indicates fluctuating lift force along the blade in this region.

1.8   Thoughs and discussion

Throughout this paper it has been shown, that it is possible to perform a three dimensional steady-state simulation of a single horizontal axis wind turbine blade to compute and visualize characteristic flow properties of a full, three bladed rotor. Although the method and geometry are rather simple, the model show good accordance to analytical calculations and the reference turbine.

A possible benefit of this method could be the visualization and optimization of more complex and unusual blade shapes, which are not able to be calculated with standard calculation software like Xfoil, as for instance the influence of leading edge protection, turbulence generators or icing on the blade.

While this method does not replace or match a transient simulation of a full rotor, it rather has to be seen as a relatively computational inexpensive preview of the overall flow characteristics.

1.9   References

Airfoiltools. (2018, 10 22). Airfoil Tools. Retrieved from Airfoil Tools: http://airfoiltools.com/

Cengel, Y. A., & Cimbala, J. M. (2014). Fluid Mechanics. Singapore: McGraw-Hill Education.

Cornell University. (2018, 10 22). Retrieved from SimCafe: https://confluence.cornell.edu/pages/viewpage.action?pageId=262012971

thewindpower.net. (2018, 10 22). The Wind Power. Retrieved from https://www.thewindpower.net/turbine_de_58_ge-energy_1.5xle.php

von Eitzen, A. (2018). Optimum circulation distribution on wind turbine rotor using the SOWFA code. Copenhagen: DTU Wind Energy.

wind-turbine-models.com. (2018, 10 22). The Wind Power. Retrieved from https://en.wind-turbine-models.com/turbines/656-general-electric-ge-1.5